# A Universal Structural Model for Human Hair to Understand the Physical Properties 2. Mechanical and Permeation Behaviors

**Masahiko Sakai, Shinobu Nagase, Tomoyuki Okada, Naoki Satoh, and Kaoru Tsujii*,#**

Tokyo Research Center, Kao Corporation, 2-1-3 Bunka, Sumida-ku, Tokyo 131-8501

(Received January 13, 2000)

The mechanical properties of human hair fiber and the permeation behaviors of some dye molecules into hair have been studied, and are here discussed based on a universal structural model proposed by the authors in the previous paper. The model consists of two structural parts, both of which have two states (Two-part/two-state model). One part of the hair, which has a higher transition temperature ($T_c$; ca. 70 °C in water), is assigned to be macrofibril and exo-cuticle; the other part with lower $T_c$ (ca. 0 °C in water) is inter-macrofibrillar materials, a cell-membrane complex (CMC) and endo-cuticle. The temperature dependence of the elastic modulus of a human hair in the Hookean region clearly shows two break points, indicating the above-mentioned transition temperatures. We have proposed a viscoelastic model based on the two-part/two-state structural model to understand the mechanical behaviors in the Hookean, yield and post-yield regions. The permeation rate of some dye molecules into hair fiber starts to dramatically increase at the higher transition temperature. Such permeation behaviors can also be understood from a universal structural model. The molecular size of dye is a crucial factor in permeation behaviors. Dye molecules with a size smaller than 1.0 nm migrate much more easily into hair.

The physical properties of human hair, such as shape-control, permeation of chemical compounds, and mechanical properties, are, of course, very important to develop various hair-care and/or hair-cosmetic products.[1] Hair properties, in principle, result from its structures. Thus, a universal structural model to understand most of the physical properties of human hair must be significantly useful for hair science as well as for developing various kinds of hair-care and -cosmetic products. In the first paper of this series, such a universal model (two-part/two-state model) for human hair structure is proposed based on experimental results of thermal- and water-setting and relaxation studies, as well as TEM observations.[2] The present paper is an extension of the previous work, and deals with applications of the proposed universal model to the mechanical properties and dye-permeation behaviors into human hair fibers.

## Experimental

**Materials.** Non-chemically treated (virgin), Japanese black and straight hair was obtained from a girl of 8 years old. The hair samples were washed with aqueous solutions of an anionic surfactant (alkyl poly(oxyethylene) sulfate type), rinsed thoroughly by deionized water and finally air-dried. A perming treatment of the hair was made in terms of immersing the hair sample for 10 min at 30 °C in a 6.0 wt% ammonium thioglycolate (mercaptoacetate) solution buffered at pH = 8.5 by $NH_3/NH_4HCO_3$, and then in 8.0 wt% sodium bromate for 10 min at 30 °C. The treated hair samples were washed twice with deionized water for 30 s, and finally air-dried.

The fluorescent dyes employed in the present study for permeation experiments are listed in Table 1, and were used without further purification. The molecular sizes shown in Table 1 were evaluated as the longest diagonal line of the smallest shadow of the projected figure, which was calculated with a computer utilizing the software package "CONCORD".[3] The reducing agent (ammonium thioglycolate) and oxidation agent (sodium bromate) were obtained from Kanto Chemical Co. and Wako Pure Chemical Industries, Ltd. respectively, and were used without further purification. Other reagents, such as urea, ethanol and inorganic salts, were purchased from Wako Pure Chemical Industries, Ltd., and were of guaranteed reagent grade.

**Mechanical Properties.** Stress-strain curves were measured with an apparatus of thermal mechanical analysis (Seiko Instruments Type-SSC/5200, TMA/SS120C module). A sample hair fiber was mounted so as to be 1.5 mm or 4 mm length, and was set in water or water/ethanol mixture (1/1 in weight) being kept at constant temperature (±0.5 °C) by circulating the thermostatic water or ethanol in the jacket of the sample holder. A solution of 2 M urea in a water/ethanol mixture ( = 1/1) was also employed as a solvent to check the effect of hydrogen bonding on the lower transition temperature (1 M = 1 mol $dm^{-3}$). The sample fiber was extended at a strain-rate of 10%/min for the usual experiments, and at a rate of 0.2—5.0%/min to separate the pure elastic and viscous terms. A same single hair fiber was used to obtain the temperature-dependence of the elastic moduli in stress-strain curves of the Hookean region, letting the hair sample recover to the original length by keeping the sample at 50 °C for 1 h after one run of the measurement was finished. Any extension of the fiber was stopped

# Present address: Japan Marine Science and Technology Center, 2-15 Natsushima-cho, Yokosuka 237-0061, Japan.

Table 1. Dye Stuffs Used in This Work

| Dye stuff | Supplier | Structure | Molecular size[a] (Å) |
|---|---|---|---|
| 7-Hydroxycoumarin-3-carboxylic acid | Lambda Probes & Diagnostics | 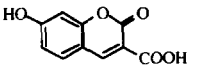 | 7.68 |
| 7-Hydroxycoumarin | Lambda Probes & Diagnostics | 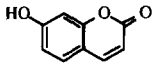 | 7.74 |
| 7-Hydroxy-4-methyl coumarin | Lambda Probes & Diagnostics | 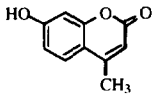 | 8.93 |
| 7-Hydroxy-3-(4-pyridyl)coumarin | Lambda Probes & Diagnostics | 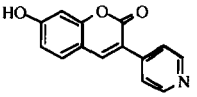 | 9.05 |
| 7-Hydroxy-*N*-methyl-quinolinium iodide | Lambda Probes & Diagnostics | 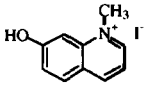 | 9.20 |
| 8-Anilinonaphthalene-1-sulfonic acid (ANS) | Wako Pure Chemical Industries, Ltd. | 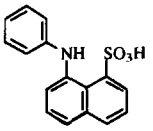 | (10) |
| 6,8-Dihydroxypyrene-1,3-disulfonic acid disodium salt | Lambda Probes & Diagnostics | 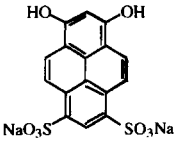 | 11.77 |
| 8-Hydroxypyrene-1,3,6-trisulfonic acid trisodium salt | Lambda Probes & Diagnostics | 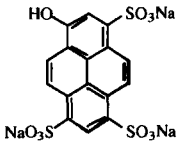 | 12.23 |
| Fluorescein | Wako Pure Chemical Industries, Ltd. | 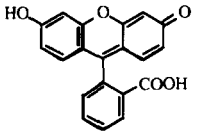 | 13.93 |
| 4′-(4,6-Dichlorotriazin-2-yl) amino fluorescein | Molecular Probes Inc. | 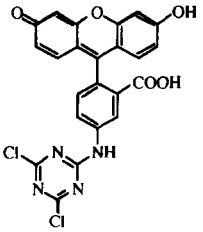 | 14.58 |
| Fluorescein succinamide | Molecular Probe & Diagnostics | 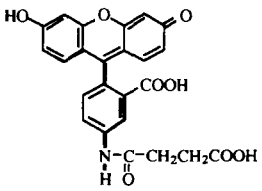 | 15.04 |

Table 1. (Continued)

| Dye stuff | Supplier | Structure | Molecular size[a] (Å) |
|---|---|---|---|
| 4′-Isothiocyanato-fluorescein (FITC) | Dojindo Lab. | 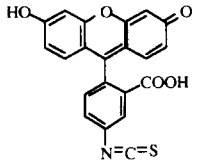 | 15.49 |
| 4′-(and 5′-)-Carboxy-fluorescein | Lambda Probes & Diagnostics | 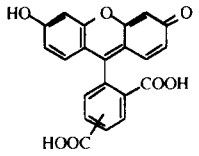 | 16.01 |
| Propidiumu iodide | Molecular Probes Inc. | 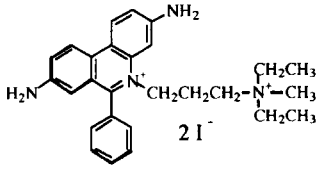 | 16.50 |
| Sulforhodamine B | Tokyo Chemical Industry Co. | 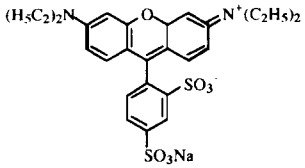 | 16.81 |
| 4′-(and 5′-)-Carboxy-X-rhodamine | Molecular Probe & Diagnostics | 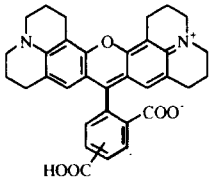 | 17.99 |

a) Computer calculation as the longest diagonal line of smallest shadow of projected figure.

before the yield region in each measurement. Full profiles of stress-strain curves up to the post-yield region were obtained using different hair fibers in each experimental run. The cross-sectional area of the hair sample was calculated from its diameter, determined using an optical microscope. An averaged value at three different points of one hair fiber was taken as the cross-sectional area of the fiber.

**Permeation Experiments of Dyes into Hair.** Permeation experiments of fluorescent dyes into hair fiber and observations of hair cross sections with a fluorescent microscope were performed by essentially the same procedures as those mentioned in a previous paper.[2] Hair fibers were immersed in an aqueous or 0.1 M buffered solutions of 1 mM dye stuff of various kinds at some different temperatures. The buffers used were lactic acid/NaOH for pH = 3 and 5, $NaH_2PO_4/Na_2HPO_4$ for pH = 7, $NH_3/NH_4HCO_3$ for pH = 8.5 and 9, $Na_2HPO_4/Na_3PO_4$ for pH = 11. Three of the hair fibers were taken out of the dye solution at appropriate intervals, and the samples were washed twice with deionized water for 30 s, and air-dried. So-dyed hair fibers were embedded in a cellulose resin, and sliced by a microtome to a thickness of 5—10 μm. A cross section of sliced hair fiber was observed, and photographed with a fluorescent microscope (Nikon type XF-EFD2). The permeation distance of the dye from the surface of the hair was determined from the photographs.

The diffusion coefficients of dye migration inside the hair fiber were calculated, assuming an infinite cylindrical shape of the hair fiber. A solution of the differential equation of diffusion for an infinite cylinder can be written as follows,[4] under the boundary conditions $C_r = 0$ at $t = 0$ and $0 < r < a$, $C_r = C_0$ at $t > 0$ and $r = a$:

$$\frac{C_r}{C_0} = 1 - 2\sum_{n=1}^{\infty} \frac{1}{\nu_n J_1(\nu_n)} e^{-\nu_n^2 Dt/a^2} J_0\left(\frac{r}{a}\nu_n\right), \quad (1)$$

where $C_r$ and $C_0$ are the dye concentrations at a distance of $r$ from the center, and the surface of the cylinder, respectively. $D$, $a$ and $t$ the diffusion coefficient of the dye, the radius of the cylinder and the time from the starting of the diffusion experiment, respectively. $J_n(x)$ is the Bessel function of the first kind of $n$th order, and is the solution of

$$x^2\frac{d^2y}{dx^2} + x - \frac{dy}{dx} + \left(x^2 - n^2\right)y = 0. \quad (2)$$

$\nu_n$ is the $n$th root of the equation $J_0(x) = 0$. The diffusion coefficients were calculated from the moving front of the dye obtained in the fluorescence microscopic photographs. The dye concentration at the front was estimated with a micro-spectrophotometer (Carl Zeiss type MPM800) to be 1/100 of $C_0$, i.e. the left-hand side in Eq. 1 at the front is 1/100. The roots ($\nu_n$) were first calculated for $n = 1$—100, and then $D$ was calculated by Eq. 1, substituting the numerical values of $a$, $a$—$r$ (distance of the dye front from the surface) and $t$. Calculations were done with a precision of $10^{-6}$ by a personal computer utilizing the Newton approximation method.

## Results

**Mechanical Measurements.** Figure 1 shows typical examples of stress-strain curves of a human hair fiber observed at temperatures below, intermediate between, and above two transition temperatures (0 and 70 °C) defined in the universal structural model.[2] Three stress-strain curves are very much different from each other. The stress values decrease remarkably with increasing temperature, and the slope (apparent elastic modulus) in the post-yield region is quite small at 90 °C. Figure 2 shows more detailed data of stress-strain curves, which can be used to analyze the temperature-dependence of the mechanical properties.

As is well known, the initial linear region up to about 3% strain is called the Hookean region. We first pay attention to this Hookean region in order to analyze the transition temperatures based on the mechanical properties. Figure 3 shows the elastic modulus (initial slope in stress-strain curve) of hair fiber in the Hookean region plotted against the temperature. It can be clearly seen that the curve has two break points at about 0 and 75 °C. These temperatures are very close to the high and low transition points observed in the hair setting and relaxation experiments.[2] It is also worth noting that the lower $T_c$ decreases upon the addition of urea. This result indicates that hydrogen bonds play an important role in the phase-transition phenomena of the low-$T_c$-part. Let us look next at the yield stress values as a function of the temperature shown in Fig. 4. We observe again a break point at ca. 0 °C. An extension at the "turn-over point" (the transition point from yield to post-yield region) and the elastic modulus

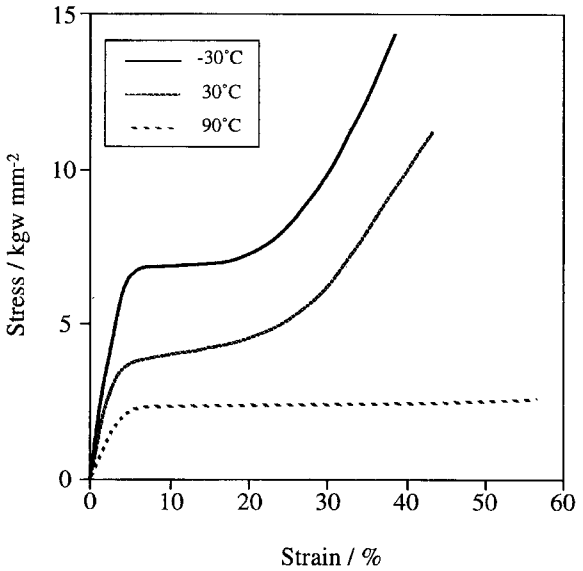


Fig. 1. Stress-strain curves of a human hair fiber observed at −30 °C (below the low $T_c$), 40 °C (intermediate between two transition temperatures) and 90 °C (above the high $T_c$). Sample hair fiber of 4 mm length for the measurement at −30 °C and 1.5 mm length for 40 and 90 °C was extended at the rate of 10%/min. Samples were set in water/ethanol mixture (1/1 in weight) for the measurement at −30 and 40 °C, and set in water at 40 and 90 °C.

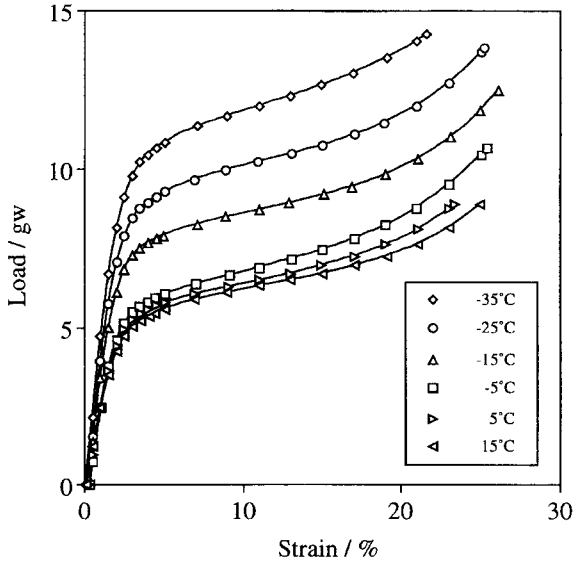


Fig. 2. Stress-strain curves of a human hair fiber observed in the temperature range covering the low $T_c$. Sample hair fiber of 4 mm length was extended at the rate of 10%/min. Samples were set in water/ethanol mixture (1/1 in weight).

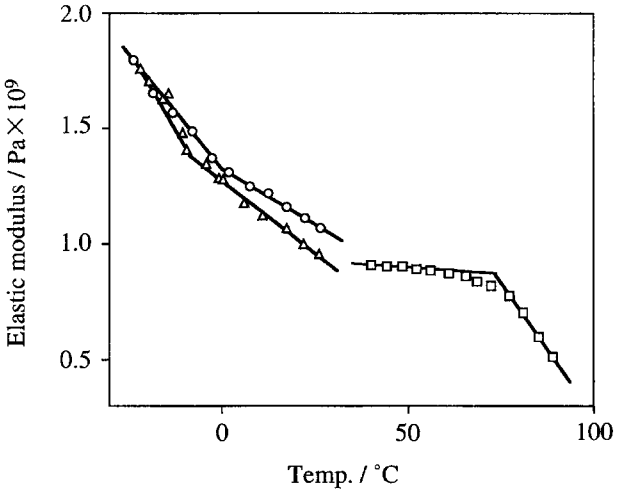


Fig. 3. Elastic modulus in Hookean region plotted against temperature. Two transition temperatures can be seen as inflection points at ca. 0 °C and ca. 75 °C. Data were taken in water/ethanol mixture (1/1 in weight) at lower temperatures (○), and in water at high temperatures (□). The moduli observed in the 2 M urea solution of water/ethanol mixed solvent are also given (△).

(slope of the stress-strain curve) in the post-yield region are plotted against the temperature in Fig. 5 to see the transition at higher $T_c$. Both curves exhibit inflections at 70—80 °C.

The elastic modulus in the Hookean region (initial slope of the stress-strain curve) contains both contributions from pure elastic and a viscous term, since the curve is measured at a finite elongation speed. In order to separate both contributions, the apparent elastic moduli obtained at several strain-rates are necessary to be extrapolated to a zero rate of strain. Figure 6 shows the dependence of the elastic modulus on the rate of strain. Only the data obtained at −30 °C

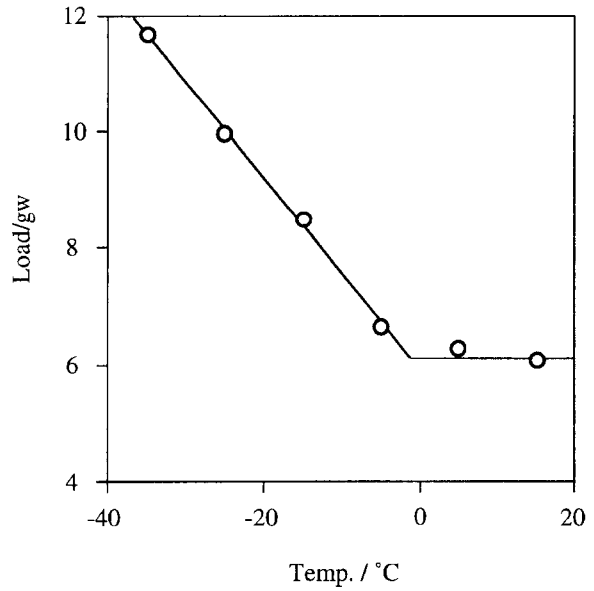


Fig. 4. Yield stress values plotted against temperature. Data are taken from Fig. 2.

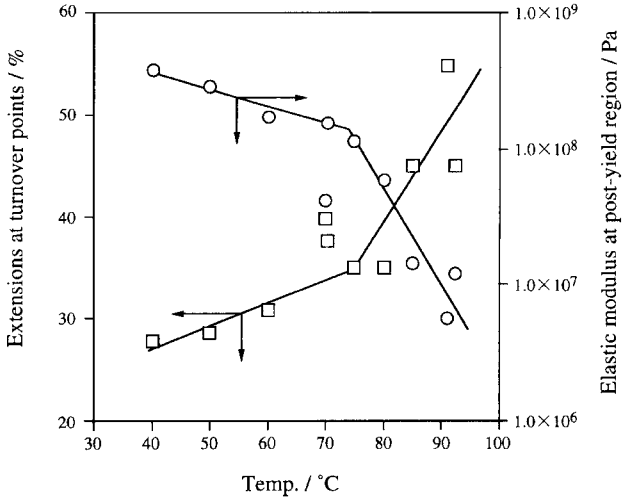


Fig. 5. Extension values at "turn-over point" and elastic moduli (slopes of the stress-strain curves) in post-yield region as a function of temperature.

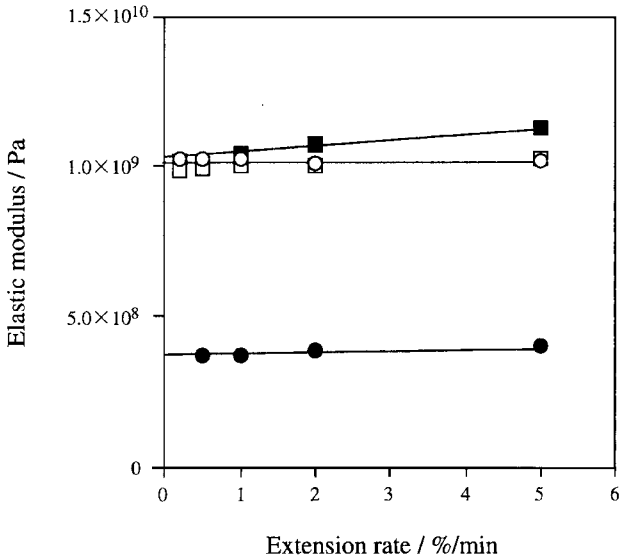


Fig. 6. Dependence of elastic modulus in Hookean region on the strain-rate measured at −30 (■) and 40 °C (□) in water/ethanol mixture (1/1 in weight), and at 40 (○) and 90 °C (●) in water.

are recognizably strain-rate dependent, which indicates that the contribution of the viscosity term in the apparent elastic modulus is large in the low-$T_c$-part. It is also evident that the pure elastic term in the low-$T_c$-part is almost zero, since the intercept value at a zero rate of strain is very close to that observed at 40 °C.

**Permeation of Fluorescent Dye into Hair.** Figure 7 shows fluorescence microscopic photographs of the cross sections of a hair, indicating a time-course of dye (Sulforhodamine B) penetration into the hair fiber. The permeation distances from the hair surface for 60 min of various kinds of dye are plotted against the molecular size of the dyes in Fig. 8a. One can clearly see that the penetration rate highly depends upon the molecular size of the dye, and a critical size of ca. 1.0 nm is present. Similar plots for the perming-treated hairs are also given in Fig. 8b. The permeation rate increases in the range of larger molecules.

The moving rate of the penetrating front of the dye in Fig. 7 allows us to calculate the diffusion coefficient of the dye molecule. The logarithm of the calculated diffusion coefficients of Sulforhodamine B (molecular size = 1.68 nm) in pure water is plotted against $1/T$ in Fig. 9. It is quite interesting to note that the diffusion coefficient suddenly jumps discontinuously at ca. 80 °C, which is close to the high $T_c$. Figure 10 shows the pH-dependence of the $\log D$ vs. $1/T$ plots for the molecular migration of Sulforhodamine B in buffer solutions. One can see an inflection at ca. 75 °C in a solution of pH = 7, which moves to lower temperatures with increasing pH. We observed one more break point in each curve at lower temperature than the above, and could not understand its significance.

## Discussion

**Two-part/Two-state Model in Hair Structures.** As discussed in our previous paper,[2] human hair consists of two structural parts, both of which have two states (Two-part/two-state model). The transition temperature ($T_c$) between the two states of one part is about 70 °C, and that of the other part is about 0 °C in a water medium. These transition temperatures highly depend upon the water content of the hair. Above the transition temperatures, both parts of the hair are soft and plastic (a melted state), and hard and elastic (a solid state) below the transition points. One part of the hair, which has a higher transition temperature, is assigned to be macrofibril and exo-cuticle consisting of keratinous proteins; the other part with lower $T_c$ consists of inter-macrofibrillar materials, cell membrane complex (CMC) and endo-cuticle of non-keratinous proteins and lipids. Both transitions at 70 °C (in the high-$T_c$-part) and 0 °C (in the low-$T_c$-part) may be a kind of gel-sol transition resulting from the breaking of

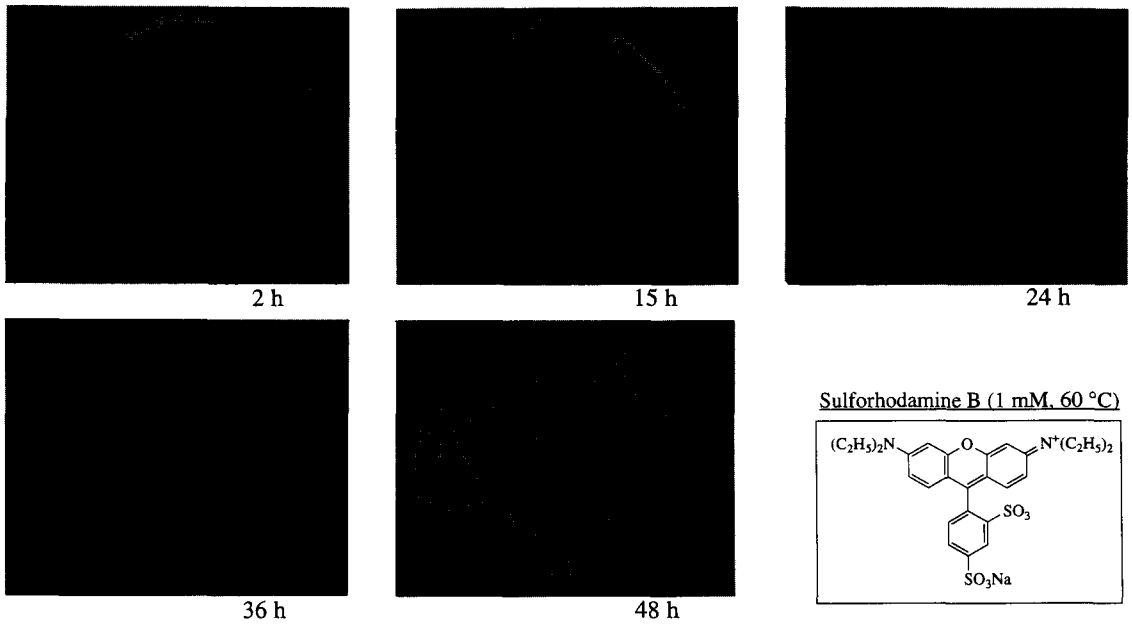


Fig. 7. Fluorescence microscopic photographs of cross sections of a hair fiber into which a fluorescent dye,Sulforhodamine B, permeates from the surface of the hair.

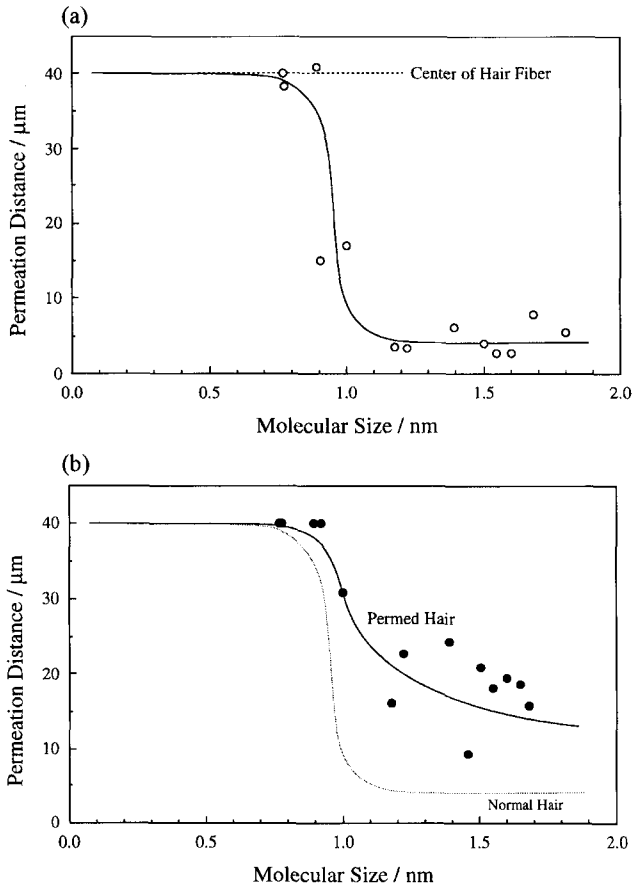


Fig. 8. Permeation distances of several kinds of dye stuff into the hair fiber from the surface of the hair for 60 min plotted against the size of the dye molecule. Data for normal hair (a) and for permed hair (b). Molecular size is estimated as the longest diagonal line of smallest shadow of projected figure (see text).

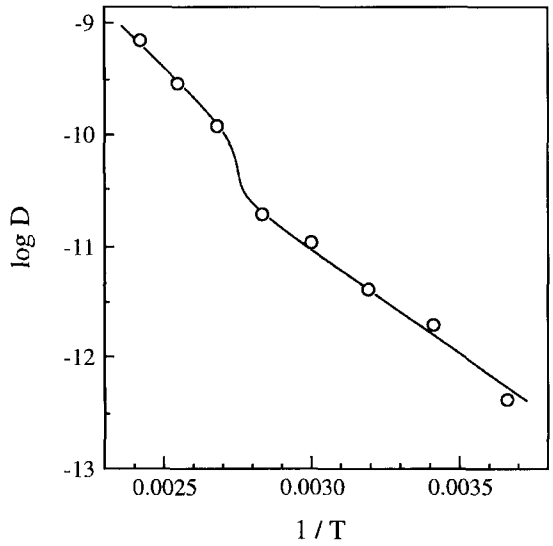


Fig. 9. The plots of $\log D$ vs. $1/T$ for Sulforhodamine B. Permeation experiments were done in pure water.

bond percolation of S–S bonds, and hydrogen and/or ionic bonds, respectively. A schematic illustration of this two-part/two-state model is drawn in Fig. 11.

The basic structural feature, which is important to analyze the mechanical and permeation behaviors, is such that the elastic macrofibrils of gel state are discretely present in the continuous soft and plastic materials of the sol state (inter-macrofibril and CMC). At higher temperatures than the high $T_c$, however, macrofibrils are also sol state, and become soft and plastic. Below the low $T_c$, on the other hand, all structures in human hair are the hard solid (gel) state. These structural images can be favorably applied to an analysis of the mechanical and permeation properties of hair.

**Mechanical Model of a Hair Fiber Based on the Two-**

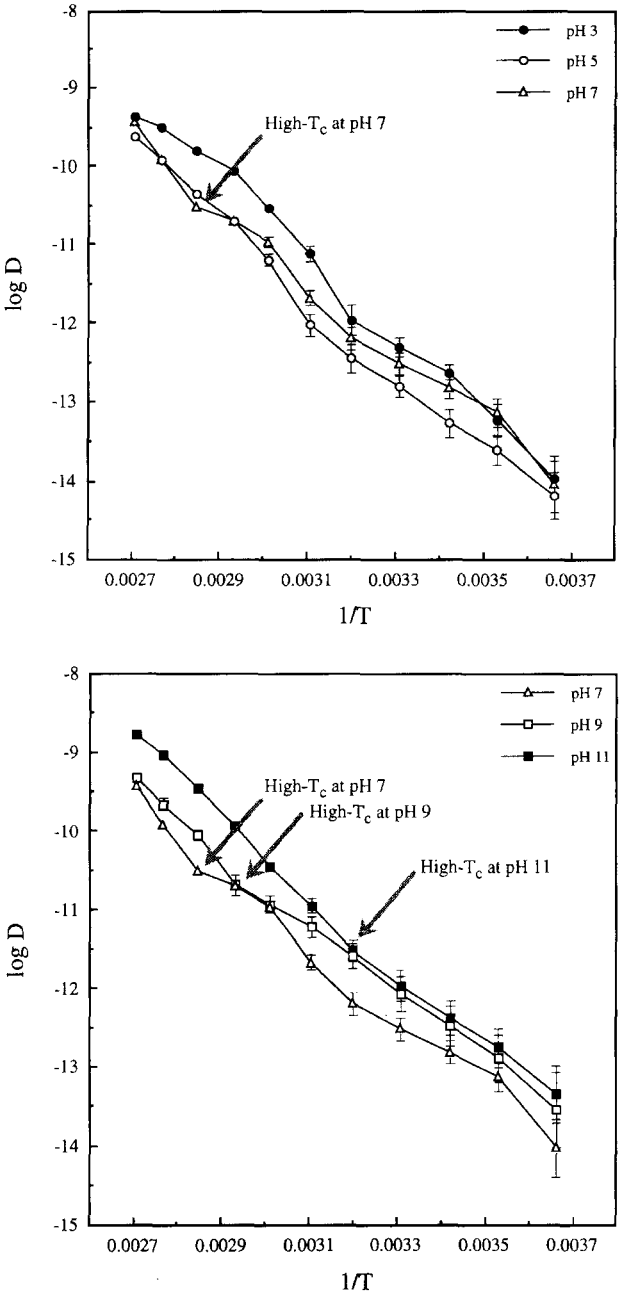


Fig. 10. pH-dependence of the log $D$ vs. $1/T$ plots for Sulforhodamine B. Aqueous buffer solutions (0.1 M) were used to keep pH values during the permeation experiments. Buffers used are lactic acid/NaOH for pH = 3 and 5, $NaH_2PO_4/Na_2HPO_4$ for pH = 7, $NH_3/NH_4HCO_3$ for pH = 8.5 and 9, $Na_2HPO_4/Na_3PO_4$ for pH = 11.

**Part/Two-State Model.** From the viewpoint of the mechanical (tensile in particular) properties, our two-part/two-state model may be represented as a combination of three viscoelastic elements, which correspond to high- and low-$T_c$-part as well as to $\alpha$-helical fibers in microfibril. In order to interpret the mechanical properties shown in Figs. 1, 2, 3, 4, 5, and 6, three mechanical elements are in parallel connection, as illustrated in Fig. 12. The low-$T_c$-part is constructed of only dashpot with no spring element, since no pure elastic

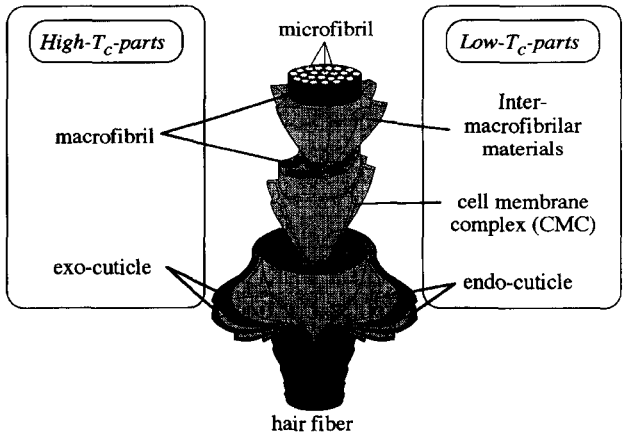


Fig. 11. Schematic illustration of the two-part/two-state model for human hair structure. High-$T_c$-parts are macrofibril and exo-cuticle, and have a transition temperature at ca. 70 °C in water medium. Low-$T_c$-parts are inter-macrofibril materials, CMC and endo-cuticle having a transition temperature of ca. 0 °C. Both parts are soft and plastic (a melted state) at higher temperatures than the transition point, and hard and elastic (a solid state) below the transition temperature.

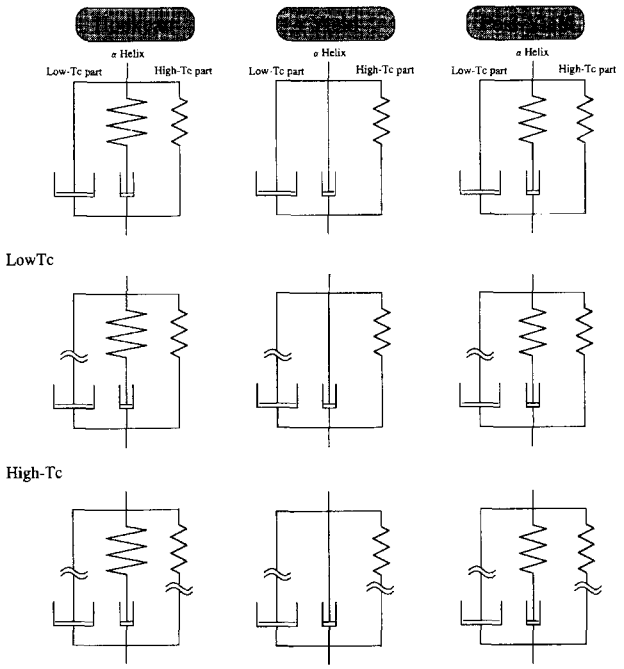


Fig. 12. Mechanical models of human hair fiber based on the universal (two-part/two-state) structural model. Three viscoelastic elements corresponding to high- and low-$T_c$-part and $\alpha$-helical structures are connected in parallel. The elements of high- and low-$T_c$-part are broken down at their gel-sol transition points. $\alpha$-helices transform into $\beta$-structure in the yield region, and do not work as springs. Sizes of springs and dashpots in the figure are qualitative indications of strength of elasticity and viscosity respectively. See text in details.

term is observed in Fig. 6. The $\alpha$-helices in the microfibril are elements of the Maxwell-type, which correspond to the mechanical behavior at 90 °C ( > high $T_c$); the high-$T_c$-part

may be a pure elastic element. In the Hookean region of the stress-strain curves, all three elements are responsible for the tensile stress at lower temperatures than the low $T_c$. At intermediate temperatures of low $T_c < T <$ high $T_c$, the low-$T_c$-part is already in the sol state and the element of this part is broken down (disconnected). When $T >$ high $T_c$, both elements of the high- and the low-$T_c$-parts break down and only the Maxwell elements ($\alpha$-helices) work. The $\alpha$-helical structure transforms to the $\beta$-form in the yield region,[5–7] and does not work as a spring in this region. The spring element of the high-$T_c$-part is disconnected at the higher transition temperature in the same manner as that in the Hookean region. At a "turn-over point" from the yield region to the post-yield region, springs come back again after a transformation from the $\alpha$-helical structure to the $\beta$-structure finishes, since the $\beta$-structure, itself, is able to act as a spring. These viscoelastic models can explain qualitatively the mechanical properties of human hair over the entire region of the stress–strain curves and temperatures.

Feughelman proposed a two-phase model to interpret the mechanical properties (particularly on the moisture effect) of keratin fibers.[6,8] The two phases in his model are $\alpha$-helices in microfibrils and the matrix part embedding them. These two phases construct the macrofibril, itself, and belong to the high-$T_c$-part in our model. From a mechanical point of view, the macrofibril ($\alpha$-helices and matrix) is not the only one viscoelastic unit, but the low-$T_c$-part (inter-macrofibrillar materials and CMC) also works as a mechanical element at temperatures lower than low $T_c$. When the experiments are conducted at ambient, and even higher, temperatures, however, Feughelman's model is reasonable, since the mechanical element of the low-$T_c$-part is always broken down. Consequently, our mechanical model is a more general one and includes Feughelman's two-phase structure.

**Viscoelastic Properties and the Gel–Sol Transition in Hair Fibers.** According to our structural model, the viscoelastic elements of the high- and low-$T_c$ parts are broken down and disconnected at their gel–sol transition temperatures. Thus, the elastic modulus and any other mechanical quantities should exhibit some remarkable change at the transition points. The elastic moduli in the Hookean region actually clearly show two transition temperatures at about 0 and 75 °C, as exhibited in Fig. 3. The effect of urea on the lower transition temperature shown in Fig. 3 strongly suggests that the hydrogen bond is a key factor to govern the transition at low $T_c$. The yield stress values as a function of temperature (Fig. 4) also substantiate the transition at ca. 0 °C. Both of extension at the "turn-over point" and the elastic modulus (slope of the stress–strain curve) in the post-yield region exhibit inflections at 70—80 °C, as shown in Fig. 5. Weigmann et al. observed the same transition at ca. 70 °C for wool[9,10] and ca. 80 °C for human hair[11] in the turn-over point extensions of the stress-strain curves. It is quite reasonable from the mechanical model in Fig. 12 that the apparent elastic modulus (including viscosity term) decreases rapidly from the higher transition temperature.

**Diffusions of Dye Molecules in a Hair Fiber of the Two-Part/Two-State Model.** According to our two-part/two-state model, a cross section of hair fiber can be schematically illustrated as Fig. 13, besides the cuticle portion. The high-$T_c$-part (macrofibril) is discretely distributed in the continuous phase of the low-$T_c$-part (inter-macrofibril materials and CMC). Let us designate the diffusion coefficients of a dye in the high- and low-$T_c$-part as $D_H$ and $D_L$, and the volume fraction (area fraction in a cross-sectional view) of high- and low-$T_c$-part as $X_H$ and $X_L$, respectively. The averaged diffusion constant ($D$) of the total system can be written as

$$D = \frac{(X_H D_H + X_L D_L)\ D_L}{X_H D_L + X_L (X_H D_H + X_L D_L)}, \tag{3}$$

where $X_H + X_L = 1$. If the diffusion of the dye occurs in a normal way, $D_H$ and $D_L$ can be expressed as

$$D_H = n_H \exp(-\Delta E_H / RT), \tag{4}$$

$$D_L = n_L \exp(-\Delta E_L / RT), \tag{5}$$

where $\Delta E_H$ and $\Delta E_L$ are the activation energies of dye diffusion in the high- and low-$T_c$ parts, respectively, and $n_H$, $n_L$ are the diffusion constants at infinite temperature. If some drastic transition takes place in the diffusion medium, on the other hand, $D_H$ and/or $D_L$ must show a discontinuous change. A sudden jump (Fig. 9) or inflections (Fig. 10) in $\log D$ vs. $1/T$ plots can be ascribed to the gel-sol transition mentioned above. The diffusion coefficient of a compound is strongly affected at the gel–sol transition when its molecular size is larger than the mesh-size of the gel.[12] This is the case in our system, since Sulforhodamin B (molecular size = 1.68 nm) is larger than the mesh-size, as shown in Fig. 8a. The decrease in the transition temperature with increasing pH value also corresponds to the previous results of hair-settings. However honestly speaking, a phase transition is not the only

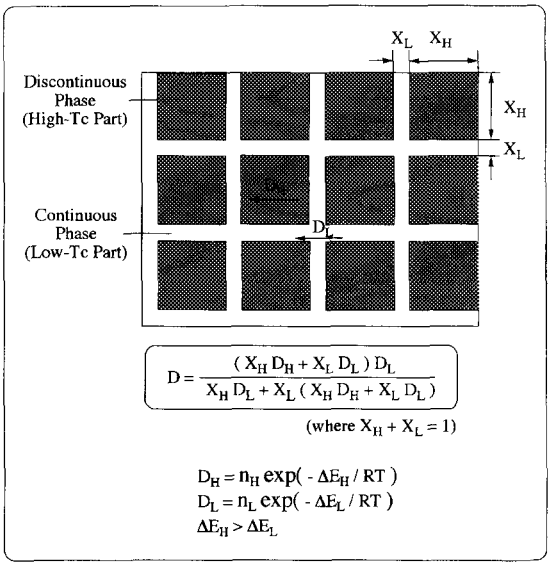


Fig. 13. Structural model for permeation into the hair fiber based on the two-part/two-state model. Cylinders of high-$T_c$-part (macrofibrils) are embedded discretely in the continuous low-$T_c$-part.

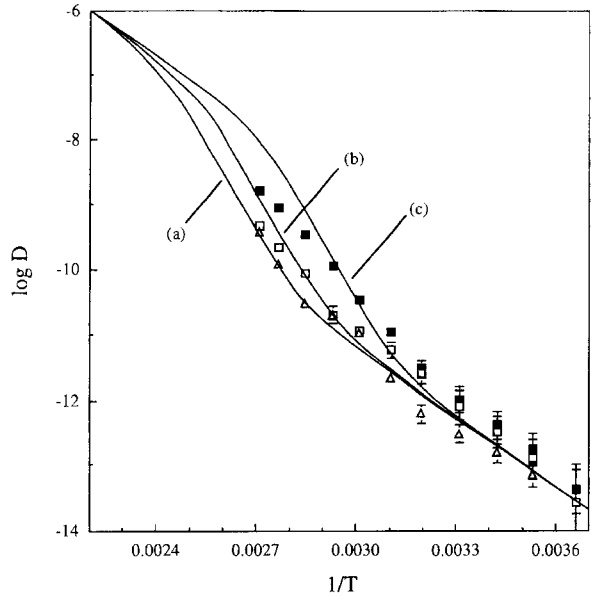


Fig. 14. Theoretical curves for $\log D$ vs. $1/T$ calculated on the basis of the structural model illustrated in Fig. 13. Parameters of $X_H$, $\Delta E_H$, $\Delta E_L$, $n_L$ are 0.938, 188 kJ mol$^{-1}$, 67.0 kJ mol$^{-1}$, 3.00 cm$^2$ s$^{-1}$ for all curves, and $n_H$ is 1.20, 6.20, $9.90\times10^{17}$ cm$^2$ s$^{-1}$, for curve (a) at pH = 7, (b) at pH = 9, and (c) at pH = 11, respectively.

explanation for the above experimental results. Theoretically calculated results using Eqs. 3, 4, and 5 are plotted in Fig. 14, assuming $\Delta E_H > \Delta E_L$. We can reproduce similar curves to Fig. 10.

**Size Effect of Dye Molecules in Their Migration into Hair Fiber.** As can be seen in Fig. 8, there is a critical size (ca. 1.0 nm) in a dye molecule to pass easily through a hair fiber. In our structural model, the high-$T_c$-part is composed of a keratin network gel with cross linkages of S–S bonds.[2] It is quite reasonable to assume that those dye molecules with a smaller size than the network mesh can easily migrate without any strong resistance. Thus, although smaller molecules than 1.0 nm may migrate in both the low- and high-$T_c$ parts, the low-$T_c$-part is the only one route for larger size molecules. A perming treatment must enlarge the mesh size of the keratin networks, because of the imperfect recovery of the S–S cross linkages in the oxidation process. The permeation behavior of larger molecules in the permed hairs could have resulted due to the above reason.

The authors express their sincere thanks to the late Professor Toyoichi Tanaka of MIT for his helpful and fruitful discussions. They also thank Dr. Junryo Mino, Head of R&D division of Kao Corporation, for his permission to publish this paper.

## References

1 C. R. Robbins, in "Chemical and Physical Behavior of Human Hair," 3rd ed, Springer-Verlag, New York (1994).

2 S. Nagase, M. Ohshika, S. Ueda, N. Satoh, and K. Tsujii, *Bull. Chem. Soc. Jpn.*, **73**, 2161 (2000).

3 R. S. Pearlman, *Chem. Des. Auto. News*, **2**, 1 (1987).

4 J. Crank, in "The Mathematics of Diffusion," Oxford University Press, London (1956), Chap. 5.

5 A. Elliott, *Text. Res. J.*, **22**, 783 (1952).

6 M. Feughelman, *J. Soc. Cosmet. Chem.*, **33**, 385 (1982).

7 H. P. Bader, in "Hair and Hair Diseases," ed by C. E. Orfanos and R. Happle, Springer-Verlag, New York (1990), pp. 60,61.

8 M. Feughelman, *Text. Res. J.*, **29**, 223 (1959).

9 H. D. Weigmann, L. Rebenfeld, and C. Dansizer, *Text. Res. J.*, **35**, 604 (1965).

10 H. D. Weigmann and L. Rebenfeld, in "The Chemistry of Sulfides," ed by A. V. Tobolsky, Interscience Publ., New York (1968), pp. 185—203.

11 L. Rebenfeld, H. D. Weigmann, and C. Dansizer, *J. Soc. Cosmet. Chem.*, **17**, 525 (1966).

12 C.-S. Kuo, R. Bansil, and C. Konak, *Macromolecules*, **28**, 768 (1995).